Counter-Ion Effects and Interfacial Properties of Aqueous Tetrabutyl Ammonium Halide Solutions

Luboš Vrbka and Pavel Jungwirth

Institute of Organic Chemistry and Biochemistry, Academy of Sciences of the Czech Republic, and Center for Complex Molecular Systems and Biomolecules, Flemingovo nam. 2, 16610 Prague 6, Czech Republic

pavel.jungwirth@uochb.cas.cz

Abstract

Aqueous solvation of tetrabutyl ammonium fluoride and iodide was investigated by means of molecular dynamics simulations in extended slab geometry. The varying propensities of the individual ions for the air/water interface were quantified and analyzed in terms of hydrophobic, polarization, and ion-ion interactions. While the cations behave as standard ionic surfactants the surface behavior of the halide counter-ions strongly depends on the ionic polarizability – iodide is surface active, while fluoride is repelled from the interface. The counter-ion effects at different concentrations on the density and charge profiles across the aqueous slab are discussed in detail.

Keywords

Ionic surfactant, counter-ion, aqueous salvation, air/water interface, molecular dynamics.

Introduction

The behavior of ions at aqueous interfaces is crucial for many physical and chemical processes in biological systems, in the atmosphere, and in technological applications. Propensities of charged species for the surface of aqueous solutions exhibit pronounced ion specificity. On one side, small hard (non-polarizable) ions, such as alkali metal cations or fluoride, are strongly repelled from the air/water interface.[1,2] On the other side, ionic surfactants, which contain strongly

hydrophobic groups (such as aliphatic chains), accumulate at the aqueous surface.[3] An interesting class of ions, which do not contain a hydrophobic group but are very soft (polarizable) exhibit an intermediate behavior with varying propensities for the air/water interface. Heavier halides (Cl^-, Br^-, and I^-), nitrate, and azide are good examples of this class.[4,5]

At finite concentrations, the counter-ion effects come into play, too. This means that the surface behavior of ions of one polarity is determined not only by their properties but also by the interfacial properties of the ions of the opposite polarity. A nice example of this effect was demonstrated in a recent study of aqueous solvation of sodium iodide and tetra-butyl ammonium iodide (TBAI).[3] Both photoelectron spectroscopy measurements and our molecular dynamics (MD) simulations show a strong effect of counter-ions on the surface propensity of iodide. I^- itself exhibits an affinity for the air/water interface with a free energy minimum at the surface of about 1-2 kcal/mol.[4] When Na^+, which is strongly repelled from the aqueous surface, is the counter-ion, it tends to move iodide by attractive Coulomb forces into the aqueous phase. As a result, I^- still exhibits a surface concentration peak, albeit smaller than deduced from the from the free energy profile of a single aqueous anion, and accompanied by sub-surface depletion of iodide anions.[6] In contrast, when an ionic surfactant such as tetrabutyl ammonium (TBA^+) is the counter-ion, it "drags" iodide even more strongly to the solution/vapor interface. As a result, the anionic and cationic concentration profiles in the interfacial region of aqueous TBAI almost coincide with each other.

The purpose of the present study is to investigate the effect of counter-ions on the surface behavior of TBA^+.[7,8] In particular we employ as counter-anions two extremes in the halide series, fluoride and iodide, asking the following questions: Does TBA^+ move F^- to the surface or does the strong affinity of fluoride for the aqueous bulk result in a creation of a surface electric double layer with cations closer to the gas phase than anions? Does the change of counter-ion from I^- to F^- influence the surface behavior of a strong surfactant such as TBA^+? What is the effect of polarization interactions, which are to a large extent responsible for the different surface propensities of I^- vs. F^-, on the distribution of ions under investigation at the solution/vapor interface

and in the aqueous bulk? In the rest of the paper we attempt to answer these questions by means of molecular dynamics simulations with the aim to obtain a detailed picture of the behavior of these ions at the aqueous surface.

Results and Discussion

We performed MD simulations of aqueous tetra-butyl ammonium solutions with iodide and fluoride as counter-ions. Iodide and fluoride were chosen intentionally. They represent two extremes on the polarizability scale – large, soft, and highly polarizable iodide (polarizability of 6.90 $Å^{-3}$) and small, hard, and almost non-polarizable fluoride (polarizability of 0.974 $Å^{-3}$).[9,10] Simulations were performed in a slab geometry, the liquid system thus possessing an aqueous bulk region in between two solution/vapor interfaces. A detailed description of system construction, nomenclature used, force field, and MD simulations setup is given in the Computational section.

Density profiles

Counter-ion effects and the role of polarizability on the distribution of ions across the aqueous slab can be best deduced from the density profiles (i.e., translational order profiles) of the studied ions. To this end, the simulation cell was divided into 0.2 Å thick slices parallel to the solution/vapor interface and the distributions of TBA^+ nitrogen atoms, the counter-anions, as well as water oxygens across the aqueous slab were averaged over the whole trajectory. The resulting plots are displayed on Figs. 1a-d (iodide as counter-ion) and 2a-d (fluoride as counter-ion), respectively.

In systems with a single and with 16 TBAI ion pairs, described by a polarizable force field, both cations and anions clearly prefer surface to the bulk solvation (see Figs. 1a and 1b). The surface affinity of the TBA^+ can be explained by a strong hydrophobic effect due to the butyl chains, which makes it a well recognized phase transfer catalyst.[7] The non-vanishing population of the TBA^+ in the bulk phase of the concentrated solution can be rationalized as follows: Upon comparing the experimentally determined full surface coverage[8] of about 1.0×10^{14} cm^{-2} with the value pertinent

to our simulation (0.9×10^{14} cm^{-2}) we see that we are in the region of a completely developed surface monolayer of TBA^+. Since ionic surfactants do not tend to form more than one layer, the excess cations then move into the bulk phase.

The propensity of iodide anion for the aqueous surface primarily due to polarization effects was reported recently.[4,6] This effect is seen in our simulations of a single TBAI ion pair in an aqueous slab, where the ions interact only weakly with each other. Within a polarizable force field model, both ions move to the solution/vapor interface. However, when polarizability is "switched off" iodide moves into the aqueous bulk, while TBA^+ stays at the surface (compare Figs. 1a and 1c).

For the system with 16 TBAI ion pairs there are also strong inter-ionic Coulombic interactions which lead to an additional accumulation of I^- close to the surface with a high density of positively charged TBA^+. However, when polarization interactions are not present in the force field, iodide anions tend to move towards the bulk region (see Fig. 1d). Consequently, the density profiles also show an increased number of cations inside the bulk phase due to strong Coulombic attraction between particles with opposite charge.

Comparison between Figs. 1 and 2 clearly shows the different behavior of the two counter-anions. While iodide is able to follow TBA^+ to the solution/air interface, this is not true for fluoride which is, as a small hard ion, strongly repelled from the surface by image forces.[11] At low concentrations (one TBA^+ and one F^-) the ions are almost independent of each other with the cation at the surface and anion in the aqueous bulk (see Fig. 2a). At high ionic concentrations the counter-anions are moved by attractive Coulomb forces exerted by the cations towards the solution/air interface but this effect does not overwhelm their strong repulsion from the surface. At the same time, in an action-reaction process, the cations are somewhat pushed towards the aqueous bulk, although the counter-ion effect cannot override their strong surface attraction (see Fig. 2b). As a result, the cationic and anionic densities are shifted with respect to each other. This results in a creation of a surface electric double layer with a positive region closer to the gas phase than the negative one.

Since fluoride anion is almost non-polarizable we expected that the density profiles would

be similar for simulations with or without polarizability interactions. This is indeed completely true for the system with a single tetra-butyl ammonium fluoride (TBAF) ion pair (compare Figs. 2a and 2c). Interestingly, for the concentrated systems there are non-negligible differences between the density profiles obtained using a polarizable and non-polarizable force field (see Figs. 2b and 2d), apparently mainly due to water polarization effects.. Namely, the omission of polarizability results in an increase of TBA^+ concentration in the aqueous bulk region.

Charge profiles

Charge distribution profiles (Figs. 3a-d for TBAI systems and Figs. 4a-d for TBAF systems) were acquired using the same approach as for the density profiles, except that instead of particle distributions, the distributions of the (full or fractional) charges assigned to the ions or atoms were monitored. Charge profiles for all the systems under investigation exhibit similar trends. There is the region of positive charge directly at the interface (+0.5 e per the surface area of 9.6 nm^2). It can be assigned mostly to water hydrogen atoms dangling out of the water slab. Charges of cations and anions present in this region of the system effectively cancel each other for TBAI. But even for TBAF, where the cationic and anionic regions do not quite overlap, there is little net charge left since the remaining excess charge is compensated by the change of orientation of water molecules. The below region of the negative charge is somewhat more influenced by the ion distribution. A sharp negative peak (-0.5 e per the surface area of 9.6 nm^2) can be observed for all simulations with polarizable potentials and for all systems with a single ion pair. Profiles for non-polarizable simulations with high ion densities in this region are more influenced by the changed population of the ions at the interface, compared to results with a polarizable force field (compare Figs. 3b and 3d). The total charge density inside the bulk phase oscillates around zero. The oscillations are most pronounced for the 16 TBAF ion pairs system with a non-polarizable force field, where large amounts of the cations are present in the bulk phase (Fig. 4d).

It is necessary to stress that the reported charge fluctuations are very small. Observed differences are only fractions of the elementary charge per the whole slab area. When compared for

example to the partial charge assigned to water oxygen atoms (-0.73 e for the polarizable force field) it is clear that we are observing an excess of only the fraction of a single atomic charge. However, despite their small values, these charge profiles are consistently reproducible in the simulations. It can be concluded that polarization and counter-ion effects do not dramatically change the charge profiles right at the surface of the studied systems, however, the sub-surfaces and bulk regions are affected due to changes in the ion distributions.

Induced dipoles

The size and orientation of induced dipoles are strongly influenced by the distribution of ions. For systems with single TBAI ion pair, water and iodide are polarized such that the total induced dipole is oriented in the direction cation-to-anion, to compensate for the permanent dipole moment of the opposite orientation, caused by the non-uniform ion distribution. (see Fig. 5a). Also note that the induced dipole on the cation is negligible. System with a single TBAF ion pair also possess the induced dipole in the same direction, but since fluoride anions are populated inside the bulk phase, the induced dipole goes to zero near the center of the slab. In this case, the polarization comes almost exclusively from the water molecules, dipoles arising from polarization of F^- and TBA^+ being negligible (Fig. 5c). In the dilute systems, surfaces, which are anion-free, exhibit additional induced dipoles arising from the polarization of interfacial layers of water, pointing out of the slab. We observed such induced dipole also in our neat water simulations.

Systems with 16 ion pairs do not possess asymmetric ion distributions, therefore, they are not polarized throughout the whole slab in a single direction. Random orientation of water molecules in the bulk phase produces an almost zero net electric field. Resulting induced dipoles are, therefore, negligible. The largest effects can be observed in the interfacial regions. For the 16 TBAI system induced dipoles are oriented out of the water slab. Their main component is the contribution of iodide anions. On the other hand, water contributions dominate for the 16 TBAF system and the induced dipole is pointing into the water slab (compare Figs. 5b and 5d). We also performed simulations with a single TBAI ion pair with both ions on the same side of the water slab

(results not shown here). In this case, induced dipoles exhibit similar trends as for the 16 TBAI system, since there is no large permanent dipole caused by a non-uniform ion distribution along the z-axis. Induced dipole moment in the bulk is zero. The ion-free surface possess an induced dipole oriented out of the slab arising from water polarization, as discussed in the previous paragraph. The interface with ions exhibits a somewhat larger induced dipole moment thanks to polarization of the iodide anion and water molecules.

Orientation of tetrabutyl ammonium cations

Orientations of the butyl chains of the cations with respect to the normal to the air/water interface, discussed also in our previous study,[3] are almost the same for the polarizable and non-polarizable force fields and show little counter-ion specificity. All systems with a signle ion pair exhibit only a single broad peak for angles 75–150°. The butyl chains are oriented almost randomly within this range – they lay on the water surface or point into the water slab. For the systems with 16 ion pairs two peaks in the orientational profiles occur around 90° and 150°. For these concentrated systems the butyl chains are confined to more definite orientations allowing for a high number of ions to accumulate at the surface.

Conclusion

We performed molecular dynamics simulations of dilute and concentrated aqueous solution of tetrabutyl ammonium fluoride and iodide in extended systems with slab geometry. We investigated the propensities of the individual ions for the solution/vapor interface, the effect of counter-ions and of polarization interactions. While tetrabultyl ammonium cations are expelled from the aqueous bulk by hydrophobic forces, it is primarily the large value of polarizability which drives iodide to the surface, while fluoride as a hard ion is repelled from the solution/vapor interface. At high concentration the ion-ion interaction become significant and have a profound impact on the density and charge profiles across the slab.

Computational

All studied systems were constructed as follows. A box containing 863 POL3 water molecules[12] (approximate dimensions 31×31×30 $Å^3$) was elongated in the z-direction to 100 Å. Periodic boundary conditions were applied in all three dimensions to produce infinite water slab in the xy-plane with two air-water interfaces in the z-direction. A single or sixteen TBAI or TBAF ion pairs were added to the simulation cell. For the concentrated systems, 8 ion pairs were initially placed on each side of the water slab.

Potential bad contacts introduced during the build phase were removed by initial 15,000 steps long steepest descent minimization. Classical equations of motion were then solved numerically with a time step of 1 fs. Van der Waals and electrostatic interactions were cut off at 12 Å. A smooth particle mesh Ewald procedure[13] was used for accounting for the long range electrostatic interactions. All bonds involving hydrogen atoms were frozen using the SHAKE algorithm[14] . Temperature was held fixed (except for the initial heating period) at 300 K using the Berendsen temperature coupling scheme.[15] All the simulations were performed in the canonical ensemble (NVT).

After minimizations, simulations started at 10 K. During a 50 ps of heating, temperature was gradually increased to 300 K. 500 ps equilibration period followed. Finally, statistics were gathered during 1 ns production run. Coordinates and induced dipoles (for simulations with polarizable force field) were dumped every 500 steps, i.e., every 0.5 ps. Every production run thus produced 2000 frames for analysis.

MD simulations were carried out using the AMBER7 software package[16] using parm99.dat parameter set.[17] Part of the simulations was performed with polarizability included in the force field,[9] employing slightly modified anion polarizabilities.[10] A self-consistent iterative procedure was used to converge the induced dipole interaction calculation. Initial geometries using the polarizable POL3 water model were used also for non-polarizable simulations, employing the SPC/E water model[18]. These two models have the same geometric parameters, the differences are only in partial charges assigned to atoms: the charges are slightly increased in the SPC/E model

compared to POL3 in order to compensate for the missing polarizability term[18].

Acknowledgements

This work has been completed within the framework of research project Z4 055 905. We would like to thank the METAcenter Project - Supercomputer Center Brno, Westbohemian Supercomputer Center, and Supercomputer Center Prague for providing computer facilities for our work. Support for the Center of complex molecular systems and biomolecules from the Czech Ministry of Education (grant No. LN00A032) and from the US-NSF (grant CHE-0209719) is gratefully acknowledged.

References

(1) Benjamin, I. *Journal of Chemical Physics* **1991**, *95*, 3698-3709.
(2) Wilson, M. A.; Pohorille, A. *Journal of Chemical Physics* **1991**, *95*, 6005-6013.
(3) Winter, B.; Weber, R.; Schmidt, P. M.; Hertel, I. V.; Faubel, M.; Vrbka, L.; Jungwirth, P. *Journal of Physical Chemistry B* **2004**, *submitted*.
(4) Dang, L. X.; Chang, T. M. *Journal of Physical Chemistry B* **2002**, *106*, 235-238.
(5) Jungwirth, P.; Tobias, D. J. *Journal of Physical Chemistry B* **2002**, *106*, 6361-6373.
(6) Jungwirth, P.; Tobias, D. J. *Journal of Physical Chemistry B* **2001**, *105*, 10468-10472.
(7) Moberg, R.; Bokman, F.; Bohman, O.; Siegbahn, H. O. G. *Journal of the American Chemical Society* **1991**, *113*, 3663-3667.
(8) Holmberg, S.; Yuan, Z. C.; Moberg, R.; Siegbahn, H. *Journal of Electron Spectroscopy and Related Phenomena* **1988**, *47*, 27-38.
(9) Perera, L.; Berkowitz, M. L. *Journal of Chemical Physics* **1994**, *100*, 3085-3093.
(10) Markovich, G.; Perera, L.; Berkowitz, M. L.; Cheshnovsky, O. *Journal of Chemical Physics* **1996**, *105*, 2675-2685.
(11) Onsager, L.; Samaras, N. N. T. *Jornal of Chemical Physics* **1934**, *2*, 528-536.
(12) Caldwell, J.; Dang, L. X.; Kollman, P. A. *Journal of the American Chemical Society* **1990**, *112*, 9144-9147.
(13) Essmann, U.; Perera, L.; Berkowitz, M. L.; Darden, T.; Lee, H.; Pedersen, L. G. *Journal of Chemical Physics* **1995**, *103*, 8577-8593.
(14) Ryckaert, J.-P.; Ciccotti, G.; Berendsen, H. J. C. *Journal of Computational Physics* **1977**, *23*, 327.
(15) Berendsen, H. J. C.; Postma, J. P. M.; Vangunsteren, W. F.; Dinola, A.; Haak, J. R. *Journal of Chemical Physics* **1984**, *81*, 3684-3690.
(16) Case, D. A. P., D.A.; Caldwell, J.W.; Cheatham III, T.E.; Wang, J.; Ross, W.S.; Simmerling, C.L.; Darden, T.A.; Merz, K.M.; Stanton, R.V.; Cheng, A.L.; Vincent, J.J.; Crowley, M.; Tsui,V.; Gohlke, H.; Radmer, R.J.; Duan, Y.; Pitera, J.; Massova, I.; Seibel, G.L.; Singh, U.C.; Weiner, P.K.; Kollman, P.A.; Amber7, University of California: San Francisco, 2002.
(17) Wang, J. M.; Cieplak, P.; Kollman, P. A. *Journal of Computational Chemistry* **2000**, *21*, 1049-1074.
(18) Berendsen, H. J. C.; Grigera, J. R.; Straatsma, T. P. *Journal of Physical Chemistry* **1987**, *91*, 6269-6271.

Figure captions

Figs. 1a-d Density profiles for the aqueous tetrabutyl ammonium iodide: Polarizable forcefield (a) 1 pair, (b) 16 pairs, nonpolarizable forcefield (c) 1 pair, (d) 16 pairs.

Figs. 2a-d Density profiles for the aqueous tetrabutyl ammonium fluoride: Polarizable forcefield (a) 1 pair, (b) 16 pairs, nonpolarizable forcefield (c) 1 pair, (d) 16 pairs.

Figs. 3a-d Charge distribution profiles for the aqueous tetrabutyl ammonium iodide: Polarizable forcefield (a) 1 pair, (b) 16 pairs, nonpolarizable forcefield (c) 1 pair, (d) 16 pairs.

Figs. 4a-d Charge distribution profiles for the aqueous tetrabutyl ammonium fluoride: Polarizable forcefield (a) 1 pair, (b) 16 pairs, nonpolarizable forcefield (c) 1 pair, (d) 16 pairs.

Figs. 5a-d Induced dipole profiles for (a) 1, and (b) 16 aqueous tetrabutyl ammonium iodide pairs, and for (c) 1, and (d) 16 tetrabutyl ammonium fluoride pairs. Positive value for $z > 0$ and negative value for $z < 0$ indicate a dipole pointing out of the slab.

Fig. 1a

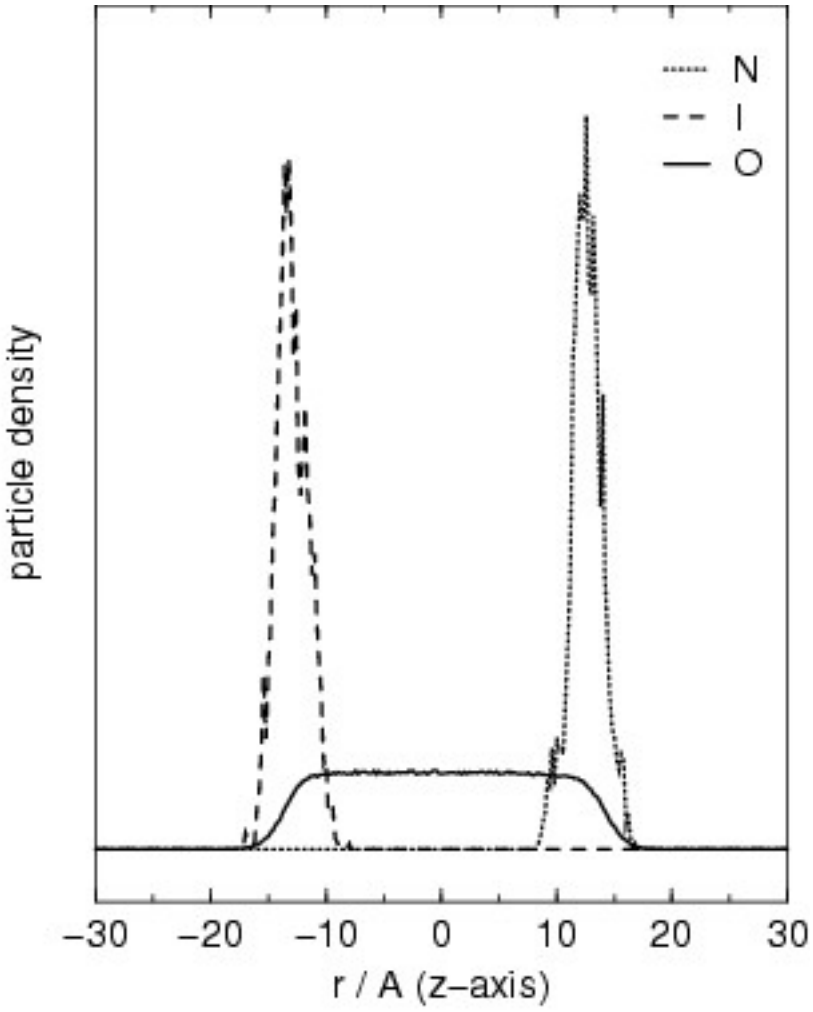

Fig. 1b

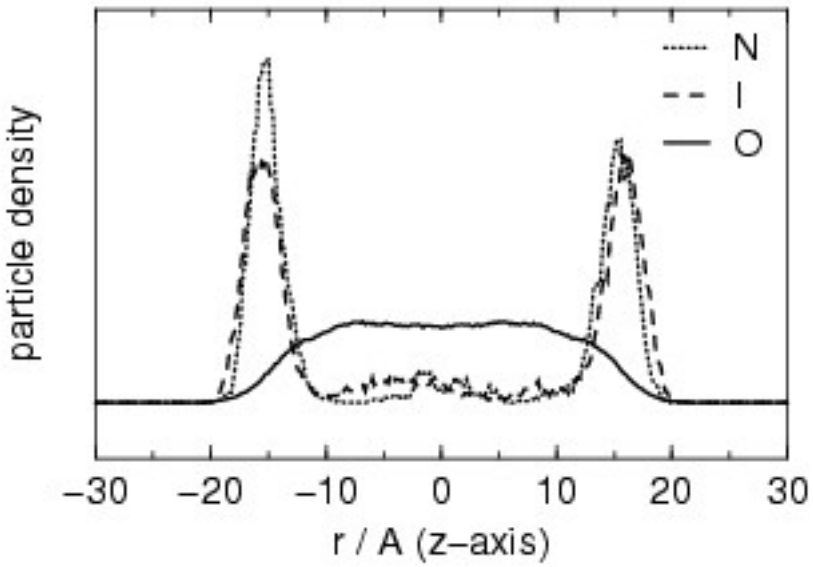

Fig. 1c

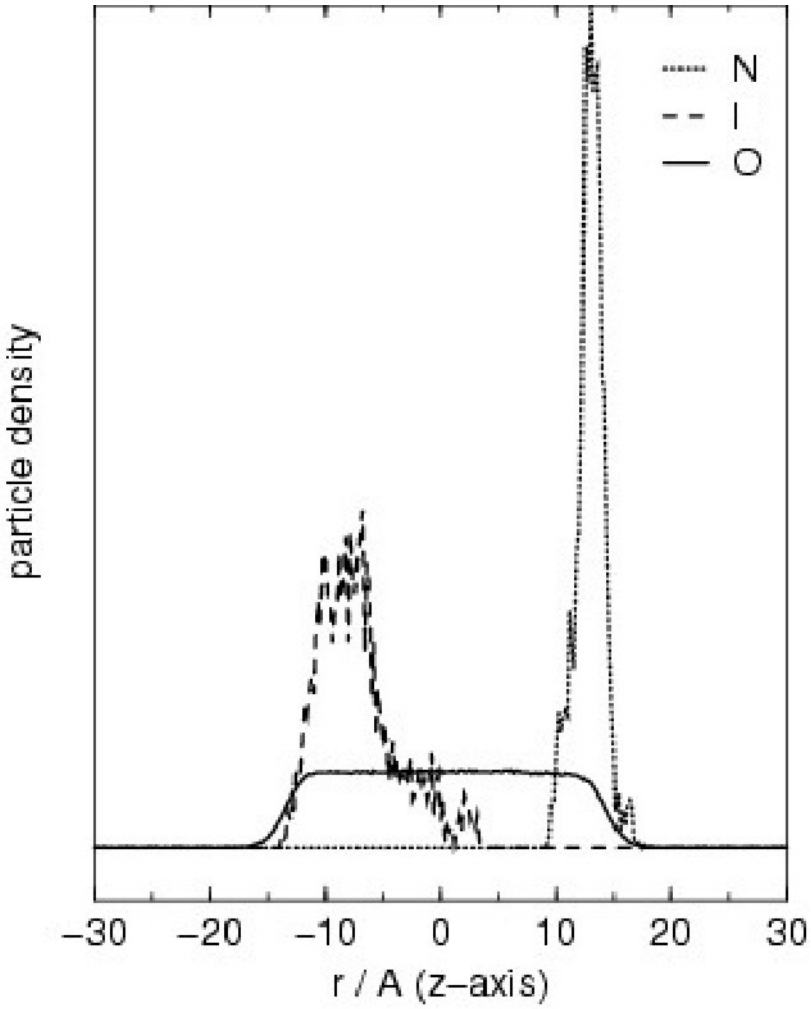

Fig. 1d

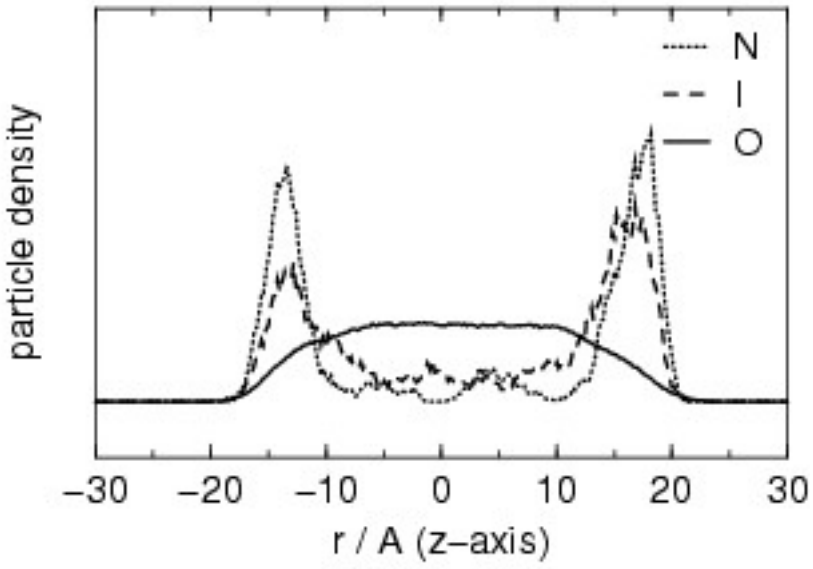

Fig. 2a

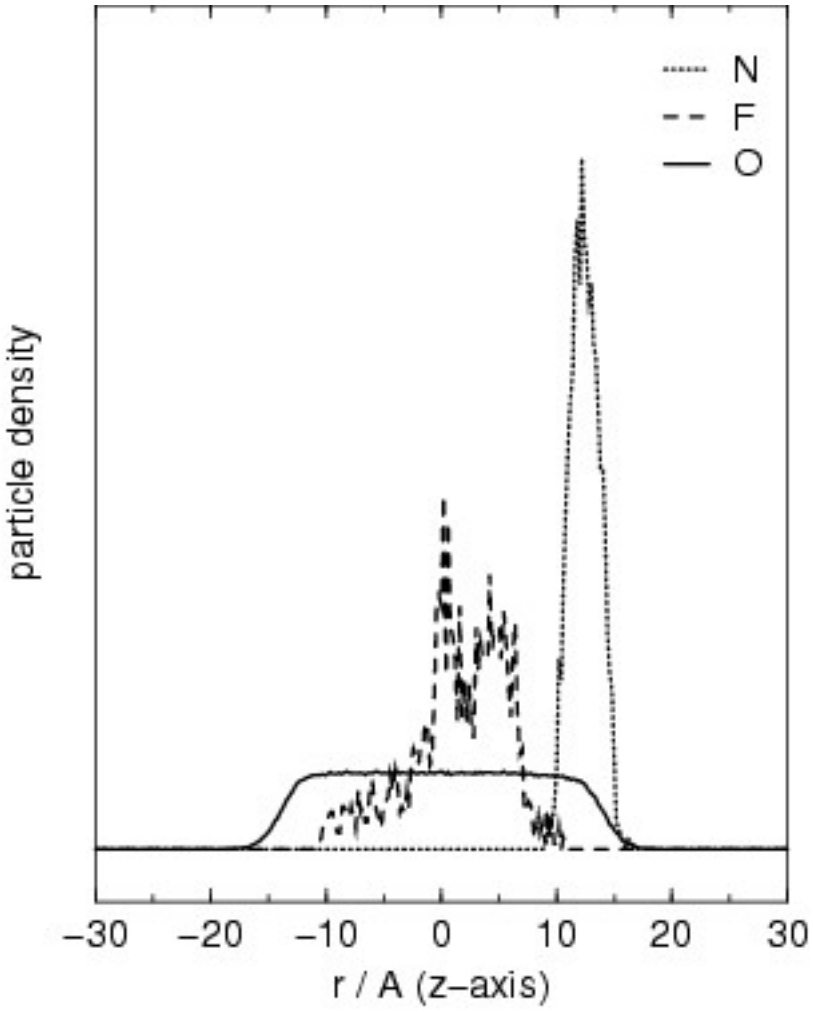

Fig. 2b

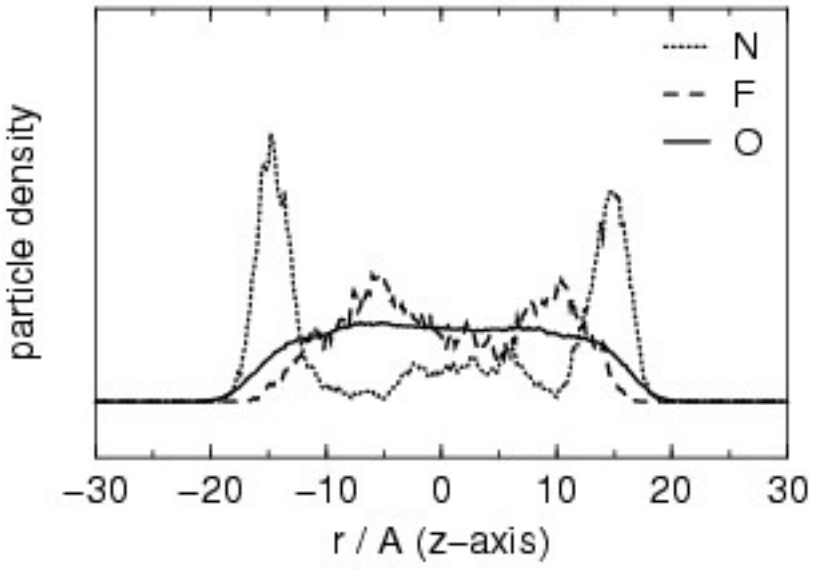

Fig. 2c

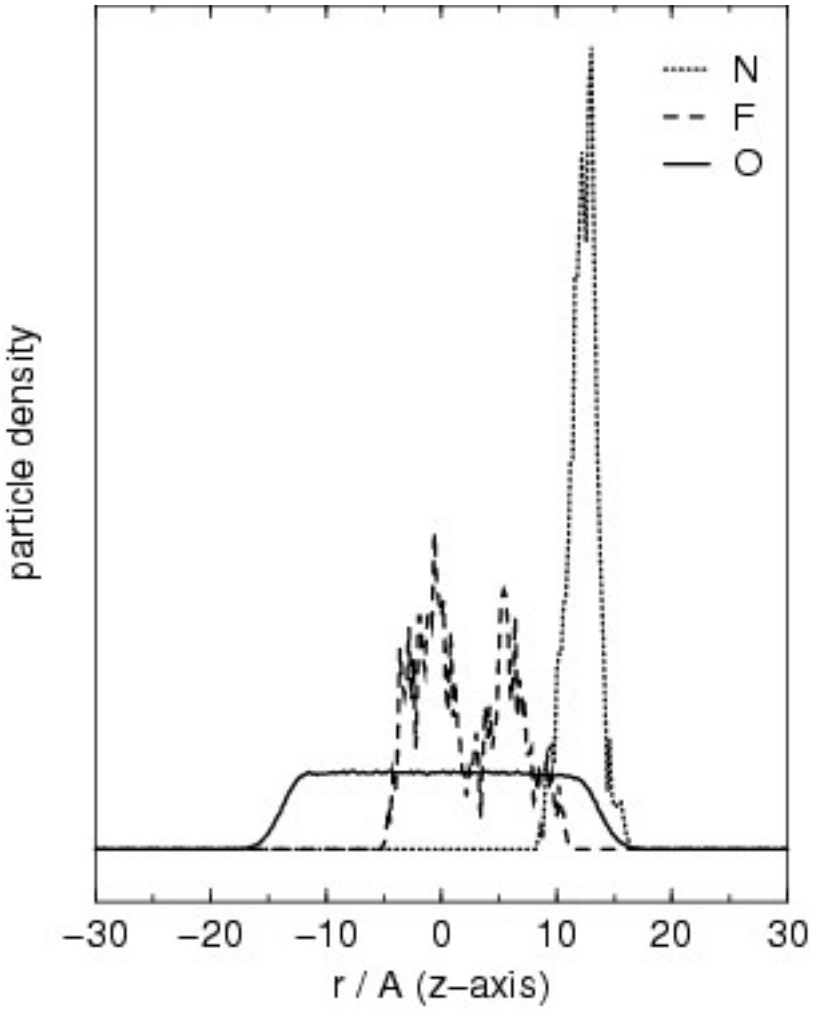

Fig. 2d

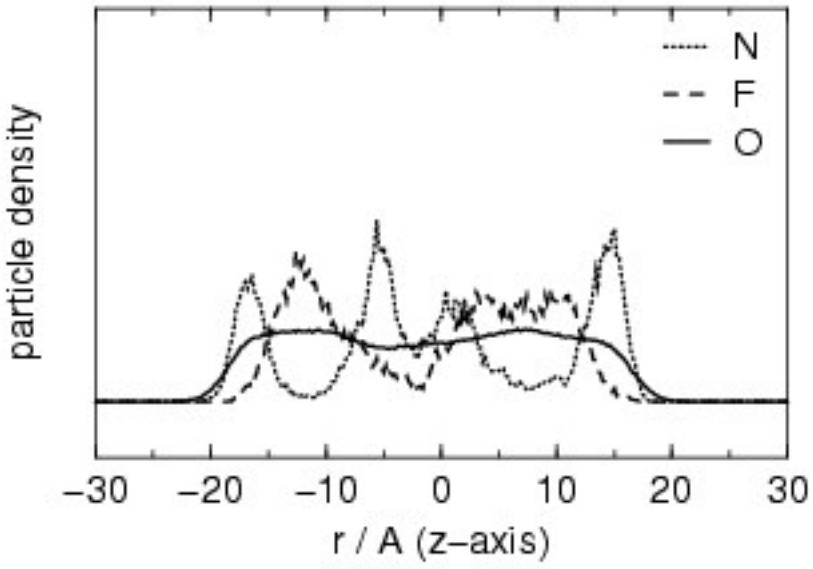

Fig. 3a

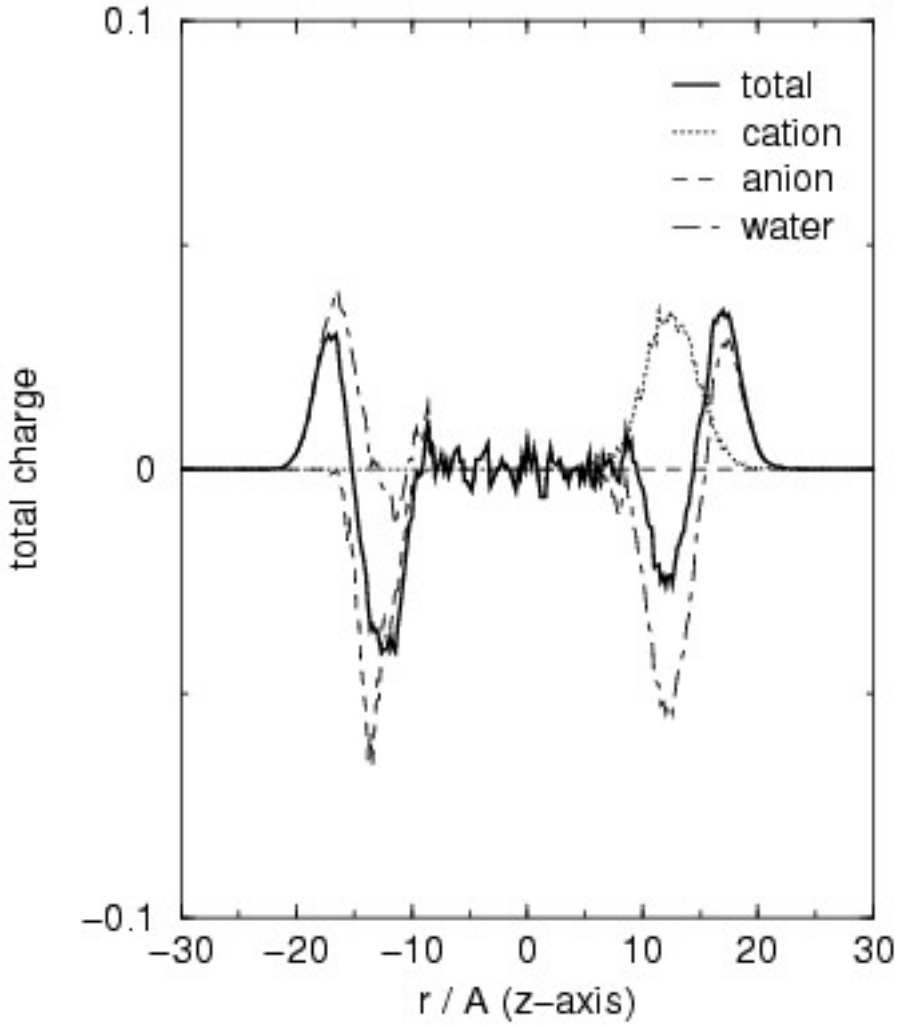
0.1
0
−0.1
total charge
−30
−20
−10
0
10
20
30
r / A (z−axis)
total
cation
anion
water

Fig. 3b

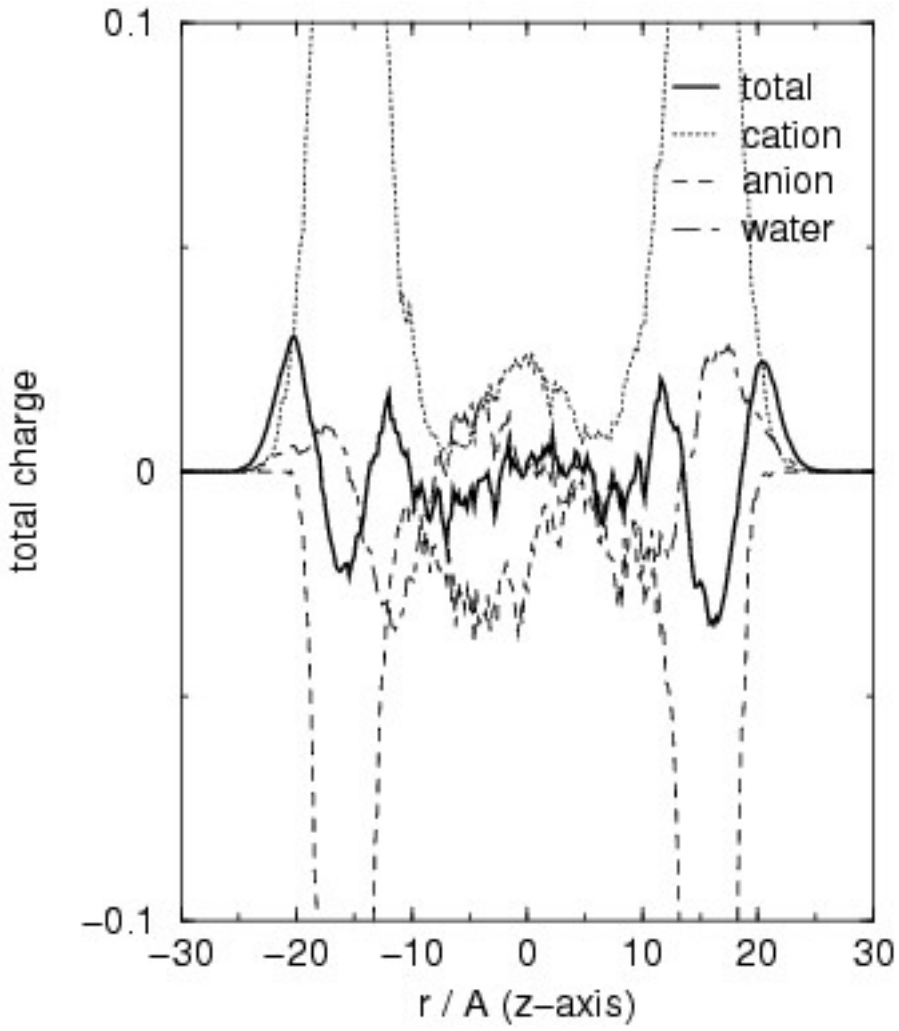
0.1
0
−0.1
total charge
−30
−20
−10
0
10
20
30
r / A (z−axis)
total
cation
anion
water

Fig. 3c

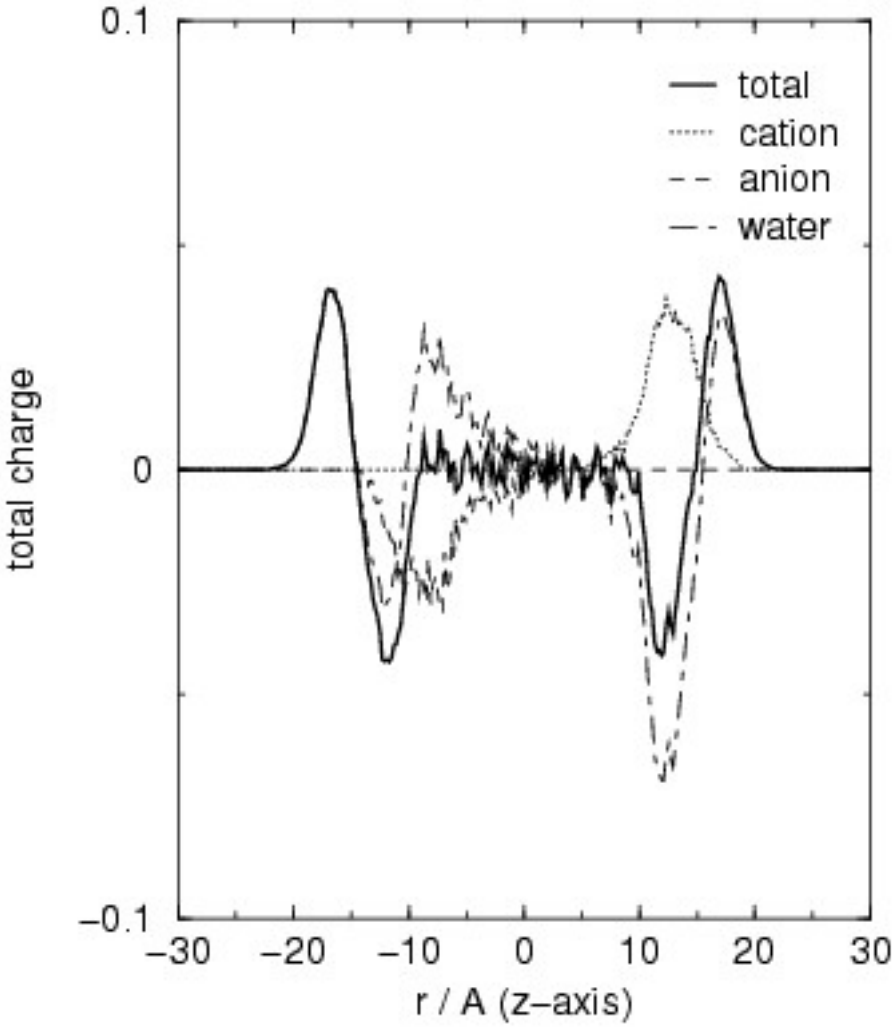
0.1
0
−0.1
total charge
−30
−20
−10
0
10
20
30
r / A (z−axis)
total
cation
anion
water

Fig. 3d

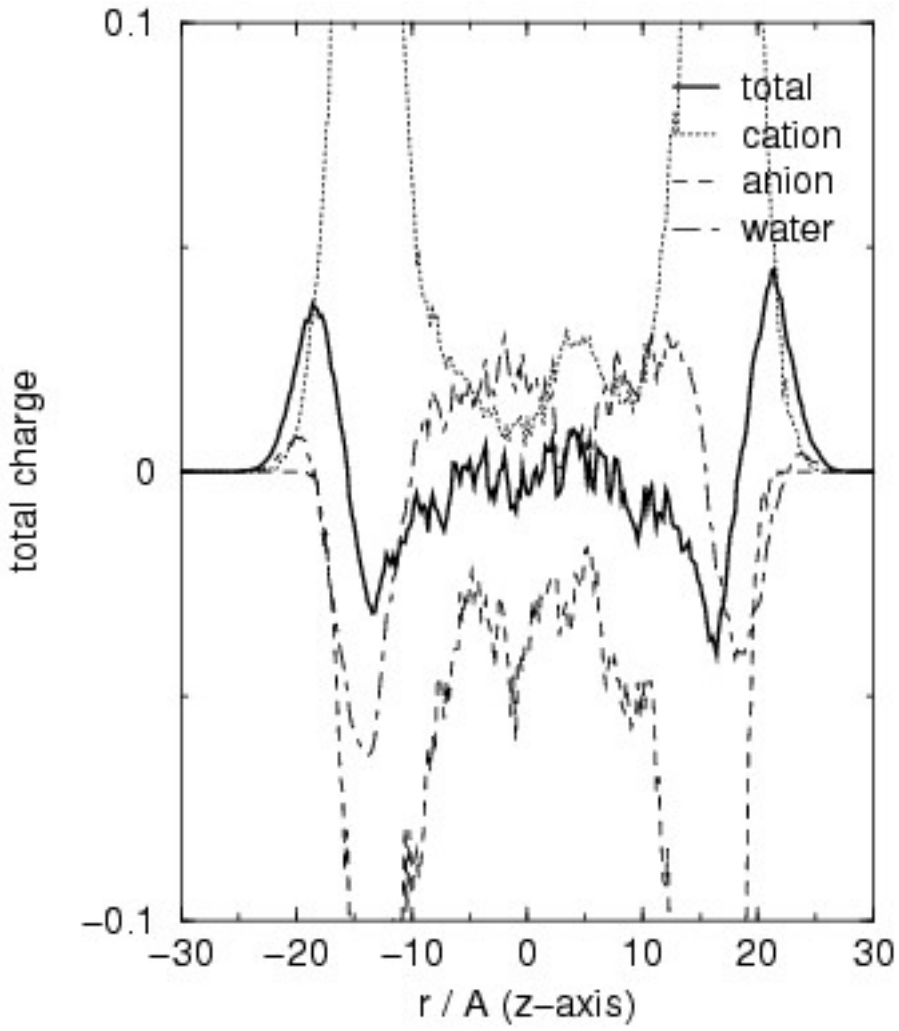
0.1
0
−0.1
total charge
−30
−20
−10
0
10
20
30
r / A (z−axis)
total
cation
anion
water

Fig. 4a

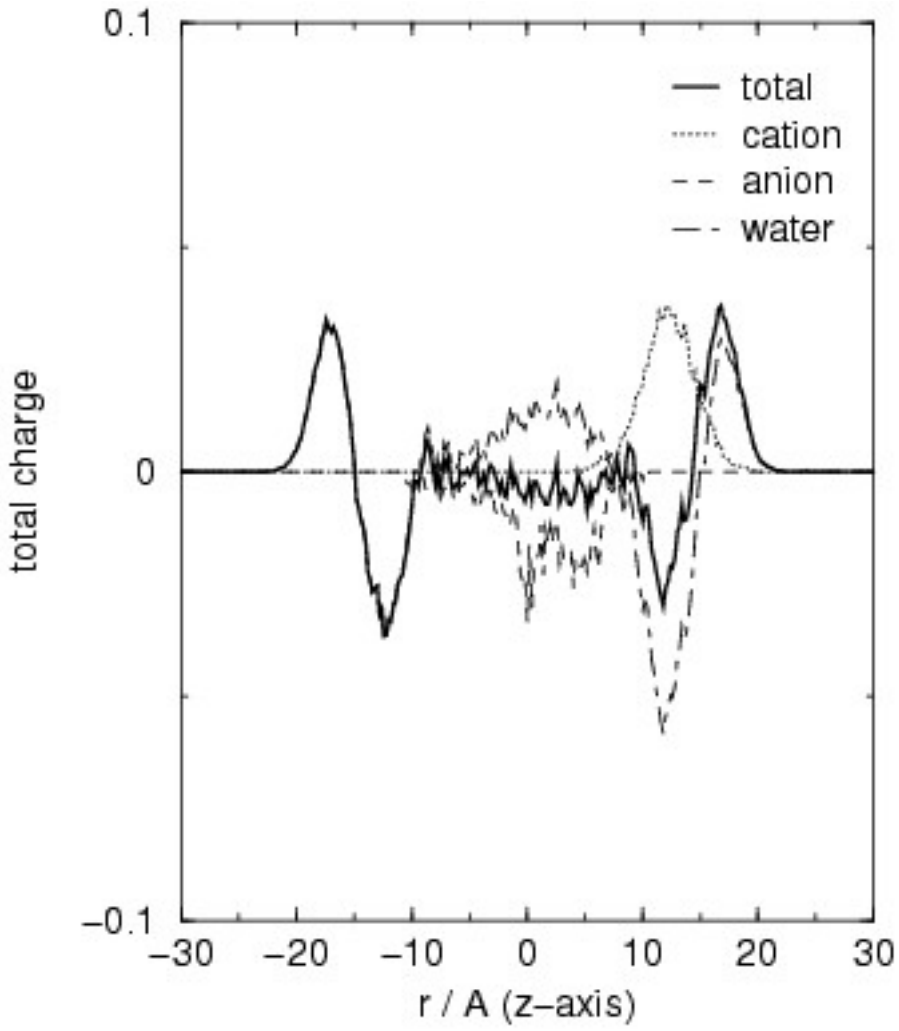
0.1
0
−0.1
total charge
−30
−20
−10
0
10
20
30
r / A (z−axis)
total
cation
anion
water

Fig. 4b

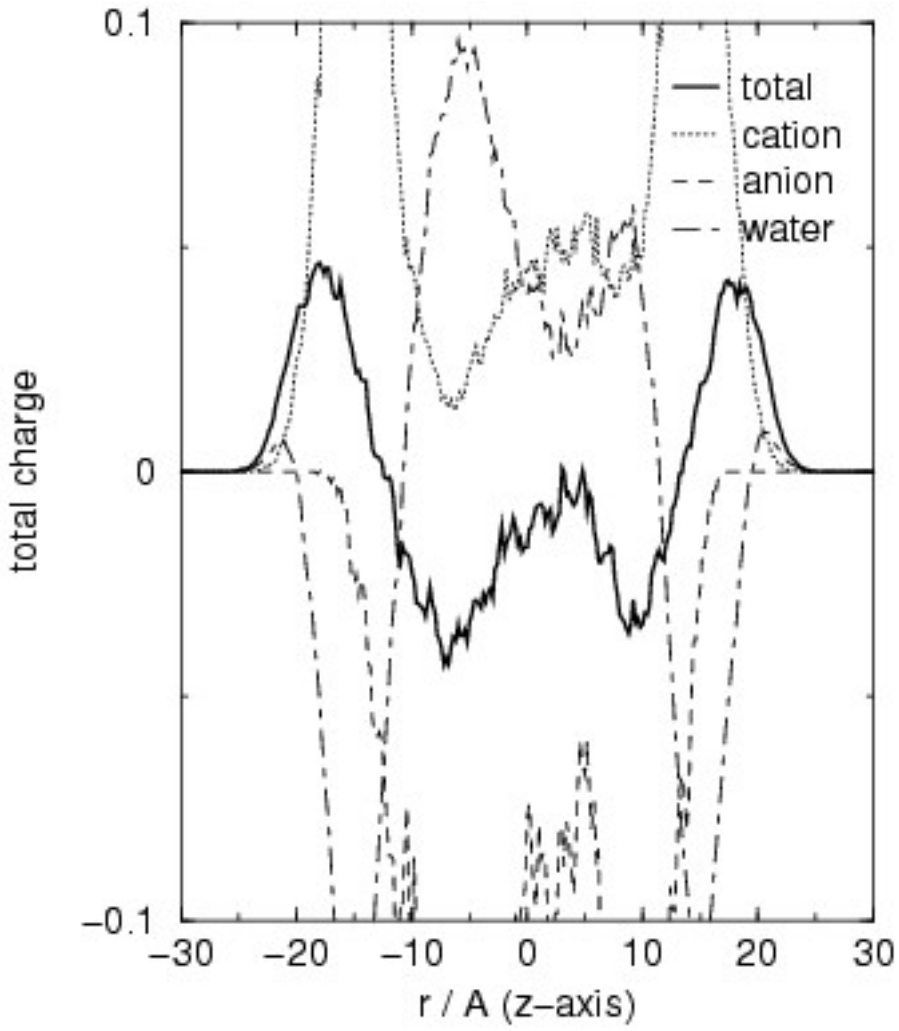
0.1
0
−0.1
total charge
−30
−20
−10
0
10
20
30
r / A (z−axis)
total
cation
anion
water

Fig. 4c

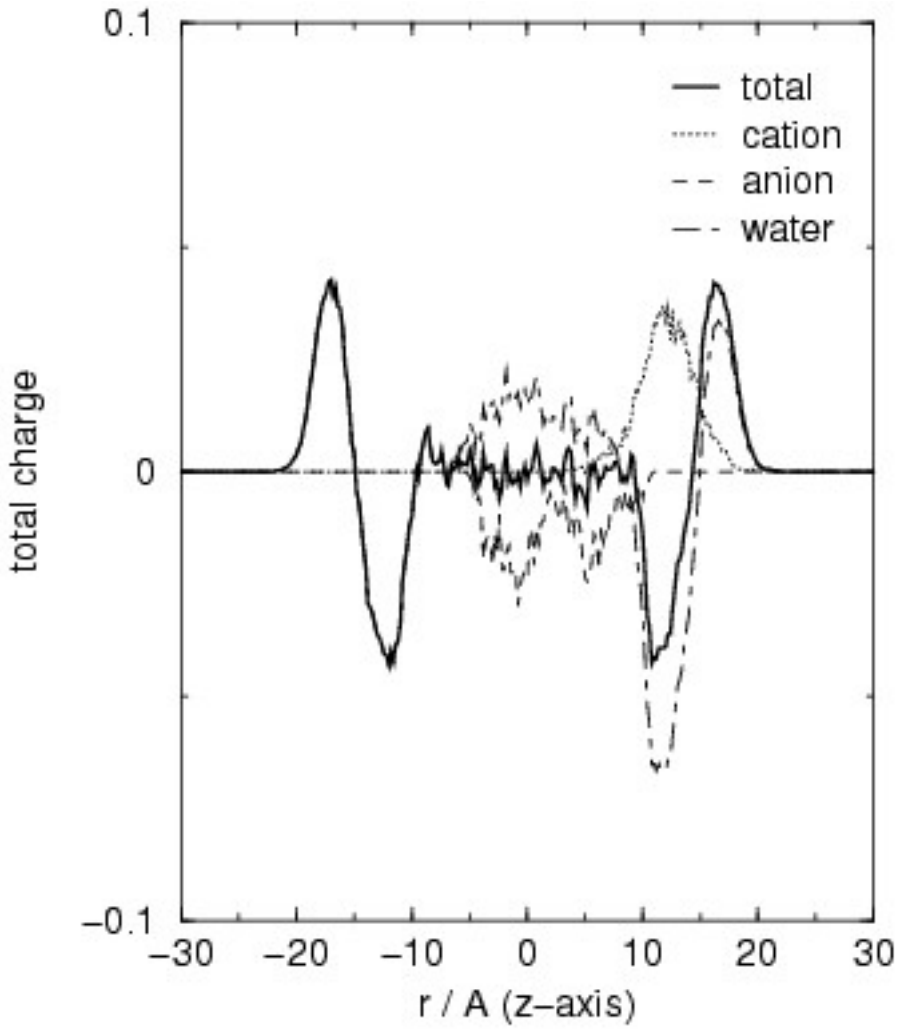
0.1
0
−0.1
total charge
−30
−20
−10
0
10
20
30
r / A (z−axis)
total
cation
anion
water

Fig. 4d

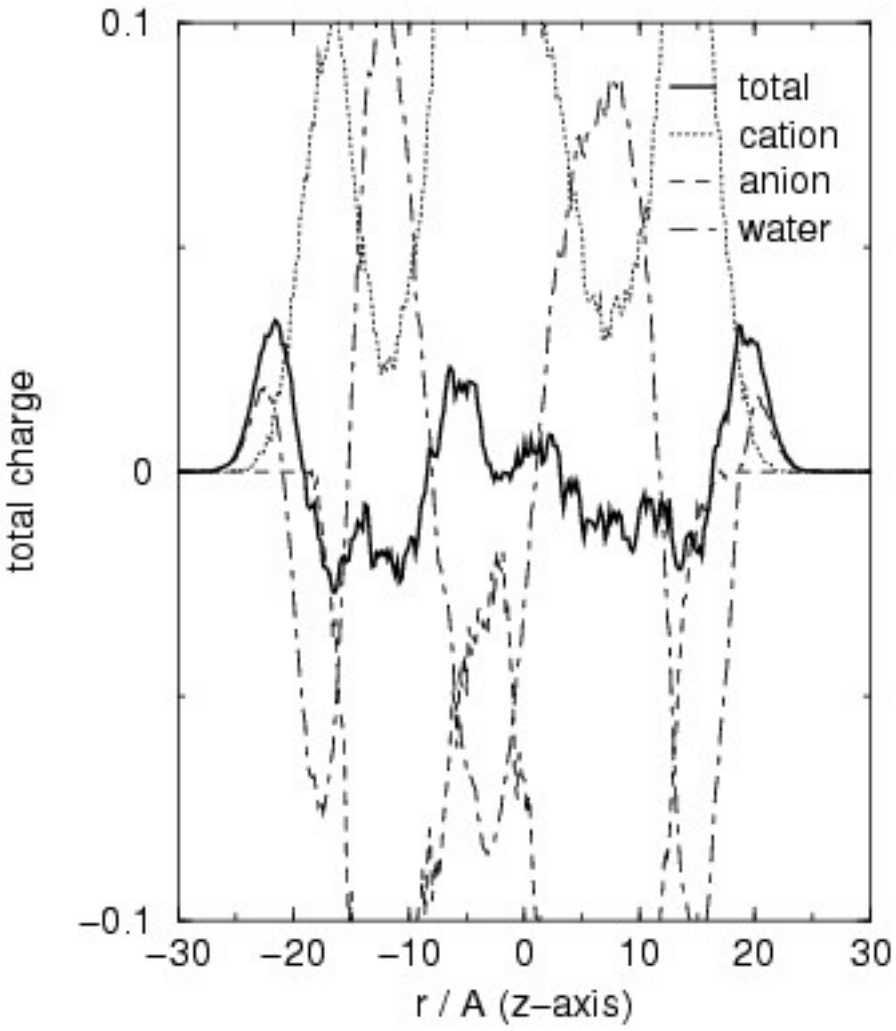
0.1
0
−0.1
total charge
−30
−20
−10
0
10
20
30
r / A (z−axis)
total
cation
anion
water

Fig. 5a

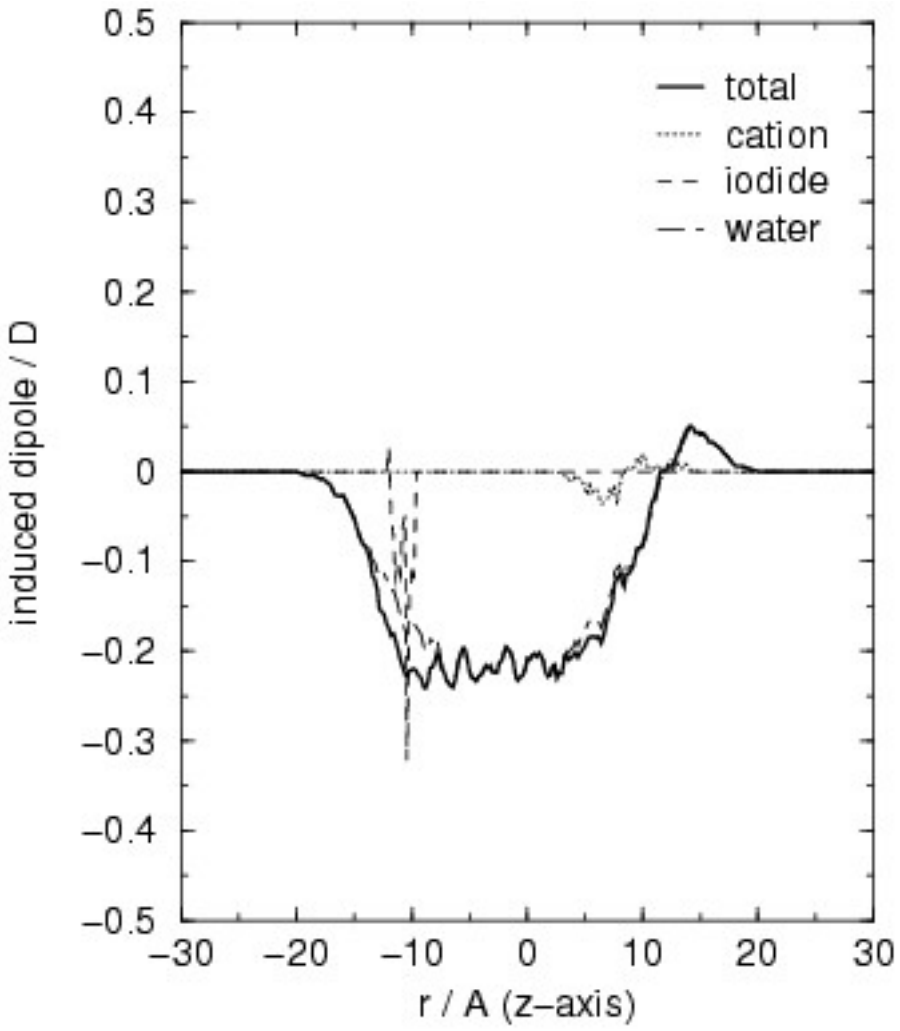
0.5
0.4
0.3
0.2
0.1
0
−0.1
−0.2
−0.3
−0.4
−0.5
−30
−20
−10
0
10
20
30
induced dipole / D
r / A (z−axis)
total
cation
iodide
water

Fig. 5b

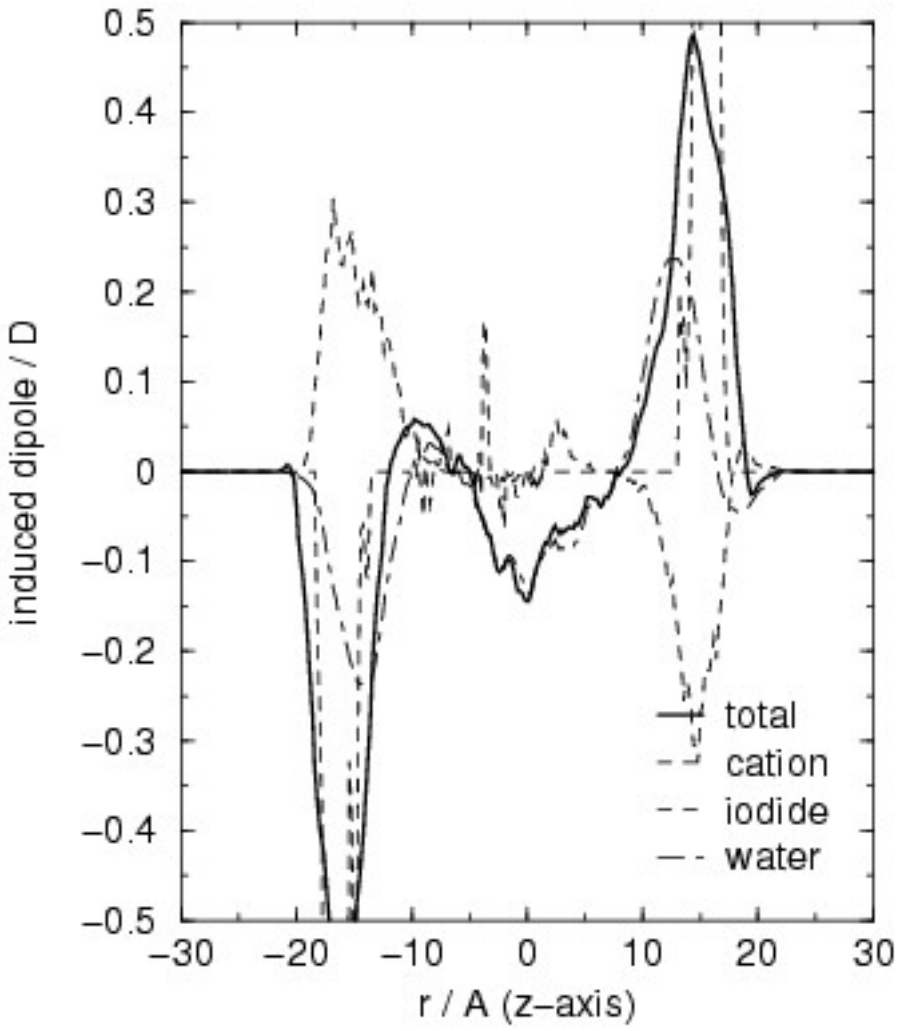
0.5
0.4
0.3
0.2
0.1
0
−0.1
−0.2
−0.3
−0.4
−0.5
induced dipole / D
−30
−20
−10
0
10
20
30
r / A (z−axis)
total
cation
iodide
water

Fig. 5c

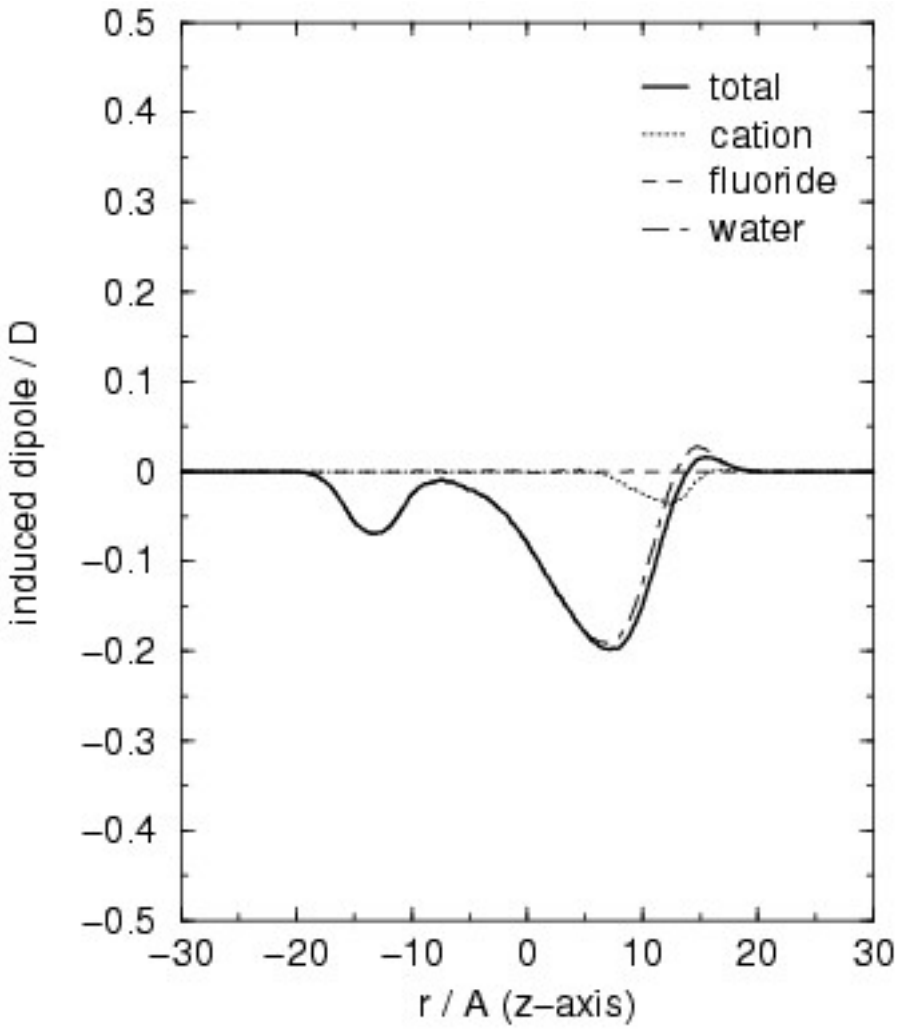
0.5
0.4
0.3
0.2
0.1
0
−0.1
−0.2
−0.3
−0.4
−0.5
−30
−20
−10
0
10
20
30
induced dipole / D
r / A (z−axis)
total
cation
fluoride
water

Fig. 5d

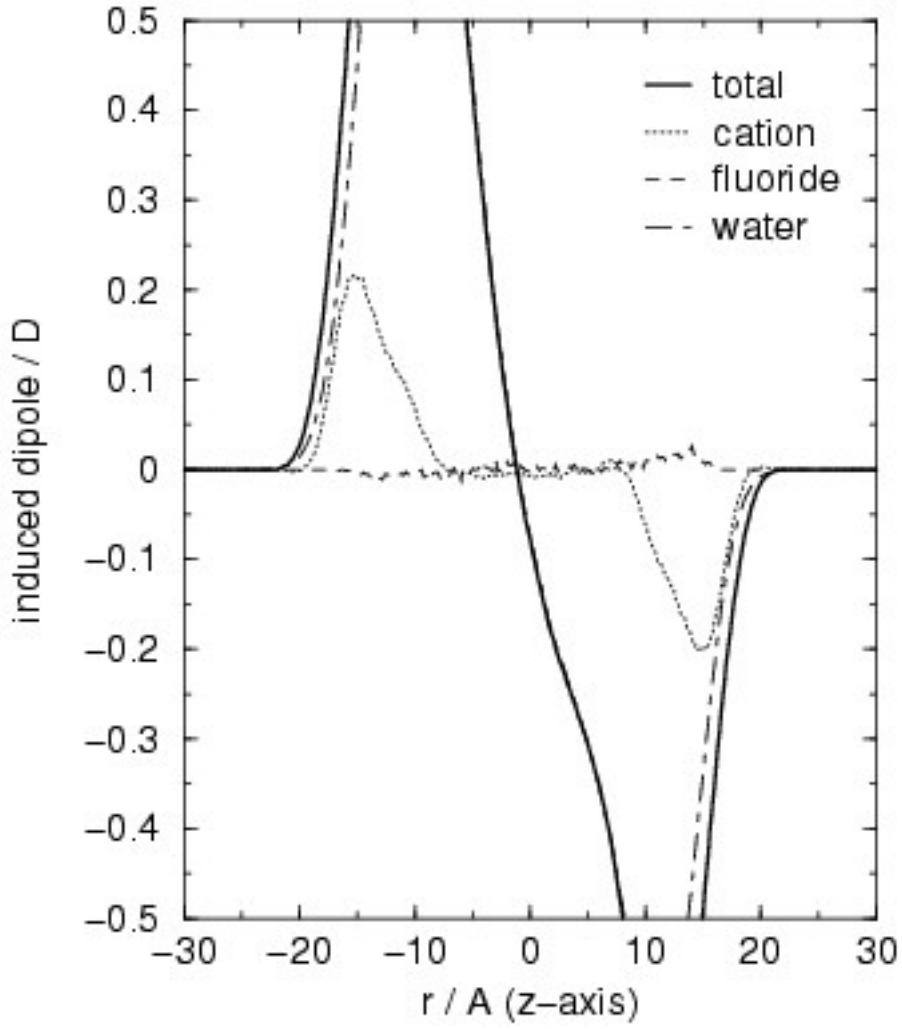
0.5
0.4
0.3
0.2
0.1
0
−0.1
−0.2
−0.3
−0.4
−0.5
−30
−20
−10
0
10
20
30
induced dipole / D
r / A (z−axis)
total
cation
fluoride
water